Modulated Magnetic Phases in Rare Earth Metallic Systems

Tapan Chattopadhyay

Neutron scattering has played a key role in the microscopic understanding of the static and dynamic properties of magnetic materials. Modulated magnetic structures first discovered in the late fifties can no longer be referred to as exotic; more than a hundred such phases have already been found in a variety of magnetic systems. Neutron and x-ray magnetic scattering have played a complementary role in the recent discovery and understanding of the modulated magnetic phases in rare earth metallic systems.

Chadwick discovered the neutron in 1932. In 1936, Bloch wrote a two-page letter (*1*) to the editor of the *Physical Review* in which he suggested that if the value of the magnetic moment of the neutron was of the same order as the known measured magnetic moment of the proton, then neutron scattering by the spin and orbital moments of magnetic atoms should be observable. Alvarez and Bloch (*2*) showed experimentally in 1940 that the neutron magnetic moment was about 0.7 of the proton value. A detailed discussion of the magnitude of magnetic neutron scattering was given by Halperin and Johnson in 1939 (*3*). Following the prediction of antiferromagnetism by Néel (*4*), Shull and Smart (*5*) provided direct experimental evidence of this phenomenon by their neutron diffraction experiment on MnO in 1949. Research on magnetic neutron scattering started with these developments and is still contributing enormously to the microscopic understanding of condensed matter.

The neutron has unique properties that render it ideal for the investigation of condensed matter. The neutron is a spin-1/2 particle that possesses a magnetic moment of 1.9132 nuclear magnetons, which can interact with the magnetic moments of atomic nuclei as well as with those of unpaired atomic electrons (*6, 7*). Thermal neutrons typically have wavelengths between 4 and 1 Å, which are comparable with the interatomic distances in condensed matter. Therefore, thermal neutrons can be used for structural (crystallographic and magnetic) investigations of condensed matter. Thermal neutrons have energies from 5 to 100 meV, comparable to those of elementary excitations (the phonon and magnon, for example) of condensed matter. Inelastic scattering of neutrons therefore enables one to study the elementary excitations of the condensed state.

The author is at the Institut Laue-Langevin, B. P. 156X, 38042 Grenoble Cedex, France, and Hochfeld Magnetlabor, Max-Planck-Institut für Festkörperforschung, B.P. 166X, 38042 Grenoble Cedex, France.

Neutron scattering techniques have been used to probe the magnetic properties of the condensed state on the microscopic scale and have given extremely useful information about the detailed spin arrangements and excitations. Recently, x-ray beams obtained from synchrotron sources have also been used to probe the magnetic properties of materials (*8*). X-ray magnetic scattering is relatively weak and only a relativistic correction to the charge or Thomson scattering. However, the magnetic contribution can be enhanced through resonance effects by tuning the x-ray energy close to that of a transition between allowed electron states in the materials.

Neutron scattering investigations during the last four decades have established that the moment configurations in magnetic materials are much more complicated than the simple ferromagnetic and two-sublattice antiferromagnetic spin arrangements predicted by Néel (*4*). Already in 1959, the first indication of more exotic helimagnetic arrangements of magnetic moments in $MnAu_2$ and MnO_2 came from neutron diffraction experiments (*9–11*). For such phases, the magnetic superlattice reflections cannot in general be indexed by multiplying the chemical cell by small integers: The magnetic periodicity is incommensurate with the periodicity of the nuclear or chemical structure. There exist also commensurately modulated long period magnetic structures. I shall refer to these two classes as modulated magnetic structures. More than a hundred such phases have already been found in a variety of magnetic systems (*12–19*). They belong to the more general class of periodically modulated physical system whose properties crucially depend on the interplay of two or more length scales. If the first scale is set by the lattice unit cell dimension, the second scale can be regarded as imposing a modulation. In modulated magnetic phases, interatomic interactions like competing exchange interactions often lead to a modulated magnetization. In this article, I shall discuss recent discoveries of modulated magnetic phases in rare earth metallic systems.

Magnetic Phases in Rare Earth Elements

The rare earth metallic elements have been the testing ground of the theories of metallic magnetism (*19*). The pioneering neutron diffraction investigations of Koehler and his co-workers (*12*) revealed what he described as "a panoply of exotic spin configurations." The crystal structures of heavy rare earth metals are hexagonal closed packed (hcp). This structure consists of the close-packed layers of atoms placed one above the other in such a way that the atoms of layer B occupy the holes formed by layer A and vice versa. After stacking layer B on layer A, one is left with two choices for stacking the third layer of atoms. One could either choose the holes of layer B just above the atoms of layer A or the rest of the holes, the corresponding stacking being referred to as A or C, respectively. The continuation of these two types of stacking infinitely produces either hcp structure (ABAB . . .) or face-centered-cubic (fcc) structure (ABCABC . . .). At room temperature, the heavy rare earth elements Gd to Lu have hcp structure with a lattice parameter ratio *c/a* somewhat smaller than the perfect value of 1.633. The lighter rare earth elements have a more complex double hexagonal structure in which the stacking sequence is ABACABAC rather than ABAB. Even more complex is the structure of Sm, which can be regarded as hexagonal with stacking sequence ABABCBCAC of nine layers.

Rare earth elements possess magnetic moments, and at low temperature, they undergo phase transitions from the paramagnetic to the ordered phase. Among the heavy rare earth elements, only Gd orders, at about 293 K, directly to a ferromagnetic structure. All other heavy rare earth elements order first to a more complicated structure, and at lower temperature, they finally undergo a further phase transition to the ferromagnetic or a conical phase. A helimagnetic structure is formed at the Néel temperature T_N in Tb, Dy, and Ho, whereas Er and Tm order with a longitudinal sine wave structure (Fig. 1). In the ordered magnetic phases, the rare earth atoms of the close-packed layers that are parallel to the crystallographic (001) plane have a ferromagnetic moment configuration, that is, the magnetic moment vectors in the close-packed layer point along the same direction.

In the helimagnetic phase, the magnetic moments in a close-packed layer lie in the (001) plane. The moment direction in the plane turns by a certain angle in going from layer to layer. The value of the turn angle depends on the periodicity of the magnetic structure, which is temperature dependent. The structure is called helical or helimagnetic because the envelope of magnetic moment vectors describes a helix in going from plane to plane along the *c* axis. The magnitude of the magnetic moment is constant in the helimagnetic phase. In the sine wave phase, on the other hand, the magnitude of the magnetic moment is sinusoidally modulated. In the sine wave magnetic phases of the rare earth elements, the moment vectors point along the *c* axis, perpendicular to the close-packed atomic layers, and are modulated in the same direction.

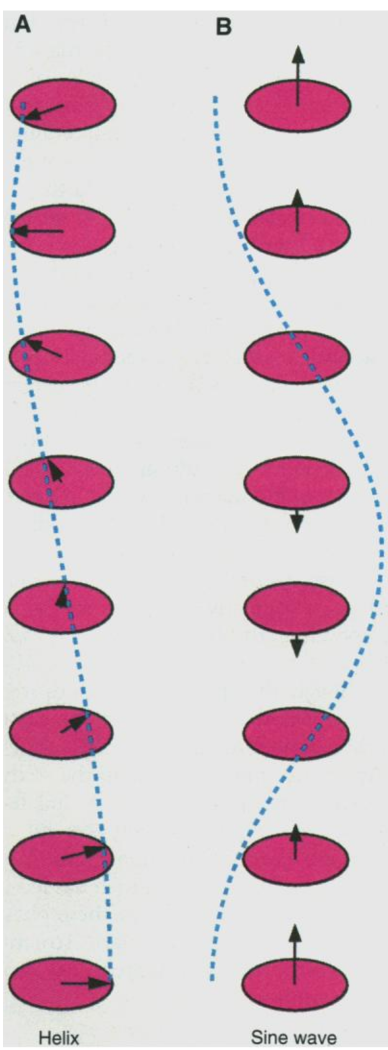

Fig. 1. Schematic representation of the two types of magnetic structures adopted by heavy rare earth metals below the ordering temperature. (**A**) Tb, Dy, and Ho order at the Néel temperature with a helimagnetic structure, whereas (**B**) a sine wave magnetic structure is formed at the Néel temperature in Er and Tm. The only exception is Gd, which orders to a ferromagnetic structure.

The periodicities of such modulated structures are generally incommensurate to the crystal structure and vary continuously with temperature. At lower temperatures, the sine wave and helimagnetic phases undergo phase transitions. The sine wave phase is only stable close to the ordering temperature and tends to become a square wave at lower temperatures because the amplitudes of the magnetic moment, which vary from site to site, tend to attain a constant value at lower temperature. Helimagnetic phases can in principle remain stable down to low temperatures because the moment on each magnetic atom can reach its saturated value. However, intraplanar anisotropy often induces phase transitions to commensurate structures. The low-temperature structures of rare earth elements are quite complicated (*19*).

Spin-Slip and Helifan Phases

Until recently, the magnetic structures of rare earth elements were considered to be known by neutron diffraction and also well-understood theoretically. Research in rare earth metallic magnetism therefore gradually shifted more toward rare earth compounds. However, the recently developed x-ray magnetic scattering technique coupled with some theoretical calculations has produced surprises. Two spin structures called spin-slip and helifan phases have been discovered recently in Ho.

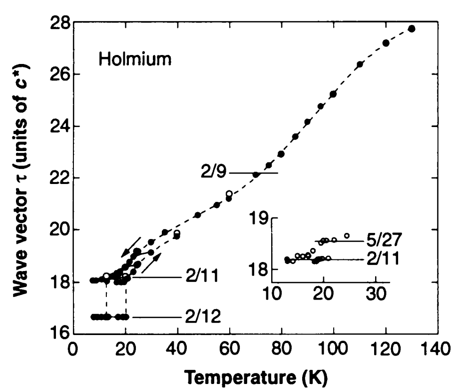

Fig. 2. Temperature dependence of the magnetic wave vector of Ho obtained by neutron (●) and x-ray (○) diffraction. Several values of k_z are marked by horizontal lines. [Reprinted from (*22*), American Institute of Physics]

The magnetic structure of Ho had been intensively investigated by neutron diffraction (*12*). Metallic Ho orders at T_N = 132 K with a simple helimagnetic structure. The magnetic moments are ferromagnetically aligned within the basal plane but rotate from plane to plane with a turn angle determined by the propagation or wave vector $\mathbf{k} = (0,0,k_z)$ of the magnetic structure (*20*). Just below the ordering temperature, the turn angle is about 50°. Because of the strong hexagonal anisotropy, the helix is drastically distorted at lower temperatures, as revealed by the appearance of higher harmonics in neutron diffraction. The wave vector decreases from about k_z = 0.275 at 132 K to 0.166 [in units of c^* (*20*)] below T = 20 K and may lock to rational values. At T = 20 K, a first-order phase transition to a conical phase (cone angle of 10°) with a net ferromagnetic moment along the *c* axis takes place. The helical component of the cone structure is commensurate with the lattice having a wave vector 2/12 (in units of c^*). The average turn angle of the spin per atomic layer is 30°, such that the magnetic spiral repeats itself every six crystallographic unit cells or 12 atomic layers. However, the presence of higher harmonics of the magnetic satellites in the neutron diffraction pattern shows that at low temperature, the spiral deviates from uniform spatial propagation. The moments are strongly bunched around the six easy directions of the basal plane crystal field.

The x-ray magnetic scattering technique has contributed to the detailed understanding of the magnetic structure of Ho (*21–23*). The excellent wave vector resolution of x-ray scattering is extremely useful for investigation of such magnetic structures. The main features of the temperature dependence of the wave vector of Ho (Fig. 2) are an inflection point around 75 K or k_z =

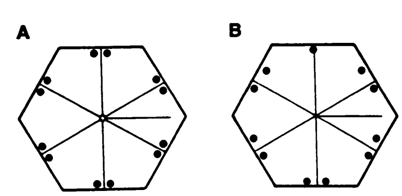

Fig. 3. A schematic and simplified drawing of the moment directions of the atomic layers in the (**A**) 12-layer zero spin-slip (2/12) and (**B**) the 11-layer one spin-slip (2/11) commensurate structures of Ho. Each circle represents the magnitude and direction of the ordered moment in a specific plane, relative to the size of the moment at 0 K (10 Bohr magnetons), indicated by the length of the horizontal lines. The orientation of moments in adjacent planes is depicted by the position of the neighboring circle. The open circle at the center in (A) represents the ferromagnetic component of the cone structure. The figure gives the results of the self-consistent mean-field calculations of Mackintosh and Jensen (*25*) but agrees generally with the spin-slip model of Gibbs *et al.* (*22*). [Reprinted from (*25*), Oxford University Press]

2/9, hysteresis below 50 K, and coexistence of phases with different wave vectors. At the lowest temperatures, a first-order phase transition takes place between the two commensurate phases with periods of 2/11 and 2/12. There are indications of a lock-in behavior near 4/2 and 5/27.

Gibbs and co-workers (*21–23*) have developed the spin-slip model of the magnetic structures of Ho. The model can be described briefly in the following way: The ferromagnetic basal planes in Ho, instead of being uniformly distributed, are arranged in pairs. Each pair is associated with one of the six easy directions, consistent with the notion of bunching, as was initially proposed by Koehler *et al.* (*12*). At 4 K in the (1/6) phase, the constant angle ϕ in the plane, between any moment and the nearest hexagonal easy axis, is only 5.8° (Fig. 3A), compared with 15°, which corresponds to a uniform helix. A spin-slip is created by associating only a single plane, instead of two, with an easy direction. For example, a single slip for five doublets will generate the magnetic structure illustrated in Fig. 3B with the wave vector (2/11). Following Gibbs *et al.* (*22*), one can denote this structure by .5, where the number of dots gives the number of spin-slips and the integer gives the number of spin doublets. It is possible to construct spin-slip structures for any rational (or irrational) wave vectors between (1/3) and (1/6). The simplest commensurate spin-slip structures are those with integer ratios of doublets and slips of .5, .4, .3, .2, and .1, the corresponding wave vectors being (2/11), (5/27), (4/21), (1/5), and (2/9). These are precisely the lock-in wave vectors found in different Ho samples.

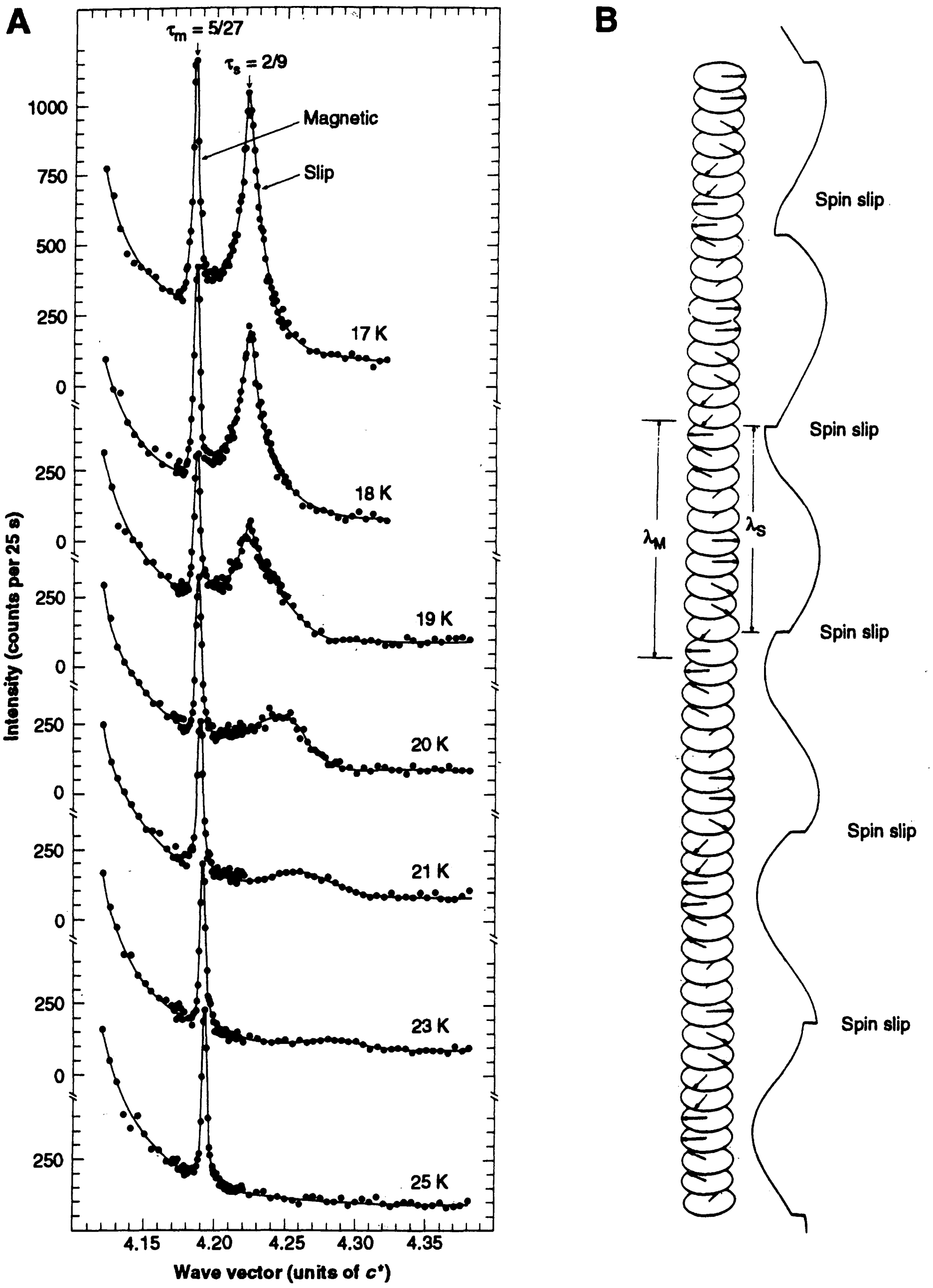

Fig. 4. (**A**) The x-ray diffraction patterns of the satellite close to the (004) reciprocal lattice point of Ho, studied for decreasing temperature from T = 25 to 17 K. In addition to the sharp magnetic satellite, a second broad satellite appears at a higher wave vector. When the temperature is lowered, the magnetic satellite approaches a wave vector (5/27), and the additional satellite becomes sharper and approaches the wave vector (2/9). The second satellite has been attributed to lattice modulation accompanying the spin slips. (**B**) A schematic drawing of the spin model. Period of complete spin of magnetic moment, λ_M; period between slips, λ_S. [Reprinted from (*23*)]

The above model with a periodic spin-slip pattern may give rise to accompanying lattice modulations from magneto-elastic interactions. For the (2/11) phase shown in Fig. 3B, the wave vector of the lattice modulation is also (2/11). For the (5/27) magnetic structure (.4.4.4.4.4.4) of Ho, there is one spin-slip for every nine atomic layers, and therefore, the corresponding interplanar lattice modulation has a wave vector (2/9). Bohr *et al.* (*23*) studied the x-ray satellites associated with the (004) reflection of Ho as a function of temperature from 25 down to 17 K (Fig. 4). Apart from the sharp magnetic satellite, a broad peak developed below 23 K, which has been associated with the accompanying lattice modulations. As the temperature was lowered, the magnetic wave vector approached the value (5/27), and the scattering caused by lattice modulation became sharper and approached (2/9). A polarization analysis of the diffraction pattern at 17 K shows that this additional peak, corresponding to the wave vector (2/9), is caused by the modulation of the charge density and is clearly distinct from the peak corresponding to the wave vector (5/27), which is of magnetic origin.

Although the spin-slip structures in Ho were discovered by x-ray magnetic scattering, there is no fundamental drawback of the neutron scattering technique in the study of these structures. In fact Cowley and Bates (*24*) have performed a very careful and extensive neutron diffraction study of the spin-slip structures of Ho, which has led to a much better understanding of these phases.

To understand the magnetic structures of Ho, Mackintosh and Jensen (*25*) used a model Hamiltonian

$$\mathcal{H} = \sum_{ilm} B_l^m O_l^m(\mathbf{J}_i) - \frac{1}{2}\sum_{ij}\sum_{\alpha\beta}\mathcal{J}^{\alpha\beta}(ij)\,\mathbf{J}_{\alpha i}\cdot\mathbf{J}_{\beta j} - g\mu_B\sum_{i}\mathbf{J}_i\cdot\mathbf{H} \qquad (1)$$

where the first term is the single-ion crystal field contribution, involving the Stevens operators O_l^m, the crystal field parameter B_l^m, and the total angular momentum **J**; the second term is the two-ion coupling, comprising an isotropic Heisenberg exchange $\mathcal{J}$ and the dipolar interaction; and the third term is the Zeeman term, dependent on a g factor, the Bohr magneton μ_B, and the magnetic field **H**. The crystal field parameters were determined primarily from a fit to the magnetic structure and magnetization curves at low temperatures. The initial values for the isotropic Heisenberg exchange were taken from the analysis of the spin waves in Ho and are strongly temperature dependent. The values were adjusted slightly to reproduce correctly the transition fields from the helical phase but remain consistent with the spin-wave data within experimental error. Results of self-consistent calculations at different temperatures agree very well with the spin-slip model.

Let us now consider the effects of the magnetic field on a helimagnetic structure. The same model Hamiltonian of Eq. 1 can be used. The effect of applying a magnetic field in the plane of the helix is first to distort the helix, giving rise to a magnetic moment along the field direction. If the field is increased, a first-order phase transition to a fan structure takes place. In the fan phase, the magnetic moments oscillate about the field direction. A further increase in the magnetic field reduces the opening angle of the fan. In the absence of magnetic anisotropy, the fan angle goes to zero continuously, leading to a second-order phase transition to a ferromagnetic phase. Hexagonal anisotropy may induce a first-order phase transition or, if the anisotropy is large, may eliminate the fan phase completely.

Koehler *et al.* (*12*) investigated by neutron diffraction the magnetic structure of Ho under a magnetic field applied in the plane of the helix. They identified two intermediate phases, which they called fan phases, and characterized them by the distribution of magnetic Bragg intensities. Magnetization and magnetoresistance measurements suggested the existence of extra magnetic phase(s) in between the helix and the fan phases. Mean-field calculations by Jensen and Mackintosh (*19, 25*) of the effect of magnetic field on commensurate periodic structures elucidated the nature of such phases.

Above about 40 K, when the hexagonal anisotropy is considerably reduced, stable phases indeed appear in Ho between the helix and the fan phases. Jensen and Mackintosh (*26*) called these helifan phases, which they described as follows: The helix may be considered as blocks of moments with components alternately parallel and antiparallel to the field, written schematically as $(+-+-+-)$, and the fan structure is described by $(++++++)$. The helifan structures then correspond to an intermediate pattern. For example, the helifan (3/2) phase, which has a relatively short period and has been found by mean-field calculations (*26*) to be the most stable over a range of fields, may be represented by $(++-++-)$ (Fig. 5).

Helifan structures represent a compromise between the demand of exchange for a periodic structure and the demand of the magnetic field for a complete alignment of moments. These phases appear when the magnetic field is applied both along the easy and the hard directions. The hexagonal anisotropy tends to suppress them. The helifan (3/2) model accounts very well for the observed neutron diffraction pattern of Ho in a magnetic field. However, both calculations and experiments suggest the existence of other helifan phases. Recently, a very careful neutron diffraction investigation (*27*) on the magnetic structure of Ho in an easy-axis magnetic field has identified the predicted helifan structures.

Jensen and Mackintosh (*19*) have rightly remarked that "the discovery of spin-slip and helifan structures in Ho has led to a remarkable renaissance in the study of the heavy rare earths, which was previously considered to be an essentially closed chapter in magnetism research." Such structures should exist in other rare earths or alloy systems and await discovery.

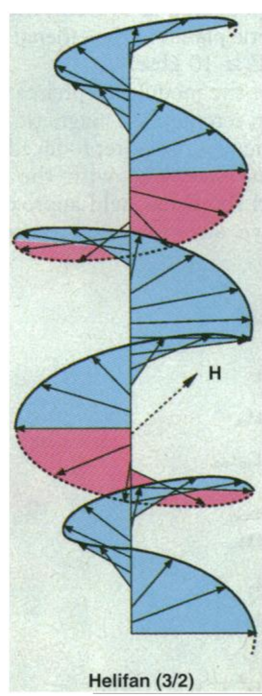

Fig. 5. The helifan (3/2) magnetic structure of Ho at 50 K. The moments lie in the plane normal to the c axis, and their relative orientations are indicated by arrows. A magnetic field of 1.1 T is applied in the basal plane, and moments with components parallel and antiparallel to the field are shown by shading with blue and red colors, respectively.

Modulated Phases Containing Nonmagnetic Planes

As mentioned, competing exchange interaction often produces modulated magnetic phases. The axial next nearest neighbor Ising (ANNNI) model (*18*) is the simplest model that incorporates competing exchange interactions appropriately. The model consists of Ising spins, $S_i = \pm 1$, situated on a d-dimensional lattice. One direction of the lattice is singled out. The interaction is anisotropic in such a way that the spins are coupled by nearest neighbor ferromagnetic interaction in a $(d - 1)$ dimensional lattice or a plane perpendicular to the axis, whereas along the axis, that is, along the direction perpendicular to the plane, the spins are coupled by ferromagnetic nearest and antiferromagnetic next nearest neighbor interactions. The important aspect of this model is the competition between the ferromagnetic and the antiferromagnetic interaction along the axis, which, together with the entropy effect, leads to a number of modulated phases with the modulation vector perpendicular to the ferromagnetic plane.

Semimetallic CeSb is perhaps the ideal system for such a model. In fact, the ANNNI model was developed by von Boehm and Bak (*28*) to explain the existence of several modulated phases in this compound. Certainly, CeSb is the most complex magnetic system ever discovered. The complexity of its phase diagram surpasses even the well-known complexity of the phase diagram of ice. It crystallizes, along with other cerium monopnictides, with the NaCl-type crystal structure and possesses unusual magnetic properties: a very small crystal field splitting, a very large magnetic anisotropy along the cube-edge directions of the NaCl-type structure, a very complex phase diagram, unusual magnetic excitation spectra, and a large sensitivity of these properties to applied hydrostatic pressure (*16, 17, 29*). However, the most remarkable and unique property of this compound is that it has several modulated phases in which nonmagnetic planes are sandwiched between ferromagnetic planes.

At zero applied magnetic field, CeSb orders at $T_N = 16.2$ K to a square-wave modulated phase with the wave vector (0, 0, 2/3) corresponding to the sequence $(+0-)$, where zero signifies a nonmagnetic plane and + and − signify oppositely oriented ferromagnetic (001) planes in which the magnetic moments are perpendicular to the plane. The magnetic phase transition at T_N is of the first order. With decreasing temperatures, CeSb undergoes five further phase transitions. The low-temperature phases are all commensurate with wave vectors (0, 0, 8/13), (0, 0, 4/7), (0, 0, 5/9), and (0, 0, 6/11) and correspond to stacking of nonmagnetic and ferromagnetic (001) planes with up or down magnetization. The ordered magnetic phase at $T \leq 8$ K is the well-known type IA phase with the wave vector (0, 0, 1/2) and a stacking sequence (++−−) of the ferromagnetic (001) planes, which does not contain any nonmagnetic (001) planes. The modulated square-wave phases containing nonmagnetic (001) planes are called antiferro-para (AFP) phases (Fig. 6). At low temperatures, a magnetic field induces two phases, called antiferro-ferro (AFF) phases, with wave vectors (0, 0, 4/7) and (0, 0, 2/3). These two phases correspond to stacking of ferromagnetic (001) planes with the sequences (++−−++−) and (++−++−). At high temperature, the magnetic field induces five so-called ferroparamagnetic (FP) phases with wave vectors (0, 0, 6/11), (0, 0, 1/2), (0, 0, 4/9), (0, 0, 2/5), and (0, 0, 1/2). These FP phases correspond to the stacking of ferromagnetic (001) planes with magnetic moments aligned along the field and paramagnetic layers. Recently, a high-field ferro-para phase FP′ with a wave vector (0, 0, 1/2) has been discovered in CeSb.

Surprisingly, CeSb does not have the well-known type I phase with ordering sequence (+−). The type I phase is the most common phase for the NaCl-type structure. However, critical scattering investigations have established the existence of anisotropic spin correlations of type I in CeSb above T_N (30). With decreasing temperature, the magnetic fluctuations increase as if the system would like to order to the type I phase, but before the long-range ordering of this structure takes place, a first-order transition to the modulated phase with sequence (+0−) occurs at T_N.

The type I phase can be stabilized in CeSb by the application of hydrostatic pressure P of only 2.5 kbar (31, 32). At $P \geq 2.5$ kbar, CeSb orders in a second-order phase transition to the type I phase, which undergoes first-order phase transitions to the modulated AFP phases. There exists a critical end point at $P = 2.5$ kbar and $T = 18$ K in the (P,T) phase diagram of CeSb at which a line of critical points corresponding to the second-order phase transitions ends on a line of first-order phase transitions. The second important effect of hydrostatic pressure is the extreme sensitivity of the Néel temperature, which increases from $T_N = 16.2$ K at $P = 1$ bar to 31 K at 21 kbar. The stability range in temperature of the AFP modulated phases decreases continuously with increasing pressure, and they disappear completely above $P = 10$ kbar. At $P \geq 10$ kbar, two completely new AF phases with the wave vectors (0, 0, 1/3) and (0, 0, 3/5) corresponding to the sequences (++−−+−) and (++−−+−−++−) of the ferromagnetic (001) planes appear between the type I and type IA phases. At these pressures, the magnetic properties of CeSb are similar to those of CeBi, which also orders in a second-order phase transition to a type I phase and undergoes a first-order transition to the type IA phase at lower temperature. As in CeBi, there are no nonmagnetic planes in the ordered phases of CeSb for $P \geq 10$ kbar.

Most of the modulated phases observed in CeSb in zero applied magnetic field and their sequences were reproduced by von Boehm and Bak (28) with the ANNNI model and the mean field approximation. There have also been some attempts to understand the details of the phase diagram of CeSb by introducing nonlinear terms in the free energy in addition to the terms of the conventional ANNNI model and that of the entropy. Nonlinear effects have been claimed to play a very important role (33, 34), making the ordered states stable at higher temperatures in large magnetic fields and giving rise to nonmagnetic planes sandwiched between ferromagnetic planes in CeSb. The origin of stability of the partially disordered state for a nonzero magnetic field $H \neq 0$ is different from that for $H = 0$. For $H = 0$, the partially disordered state originates from cancellation of the molecular field arising from neighboring spins, and therefore, the nonlinear terms are not always necessary. The cancellation of the molecular field is not expected for $H \neq 0$, and therefore, the nonlinear terms are necessary to produce partially disordered states.

The nature of the nonmagnetic planes sandwiched between the ferromagnetic layers in CeSb had been unclear until recent inelastic neutron scattering investigations (35) with polarized neutrons. Magnetic excitations in CeSb have been investigated at $H = 1.8$ T and $T = 6.5$ K in the AFF2 phase (++−−) without paramagnetic planes and at $H = 1.8$ T and $T = 15$ K in the FP2 phase (++00) with half nonmagnetic planes. The magnetic field was applied along the c axis. The full polarization analysis technique was used to measure both the spin-flip and the non-spin-flip contributions. Investigations at the reciprocal lattice vector $\mathbf{Q} = (0, -2.1, 0)$ near the zone center revealed a new peak at 3.5 meV in addition to the peak at 4.9 meV that results from magnetic excitations within the ferromagnetic planes in the FP2 phase. This new peak at 3.5 meV, which is observed in the FP2 phase with nonmagnetic planes but not in the AFF2 phase without nonmagnetic planes, has been ascribed to the magnetic excitations within the nonmagnetic planes. The polarization analysis of the magnetic excitations of the nonmagnetic planes has established that they are indeed paramagnetic planes. The new magnetic excitation is found to be dispersionless, which also suggests the paramagnetic nature of the nonmagnetic planes. This experiment has not only confirmed the existence of the nonmagnetic planes in CeSb but also has established that the nonmagnetic planes are indeed paramagnetic in nature.

The origin of the complex magnetic properties of CeSb has been attributed to the presence of the 4f level close to the Fermi level and also to the semimetallic character of CeSb. The p-f hybridization model, in which the anisotropic hybridization between the 4f states and the valence

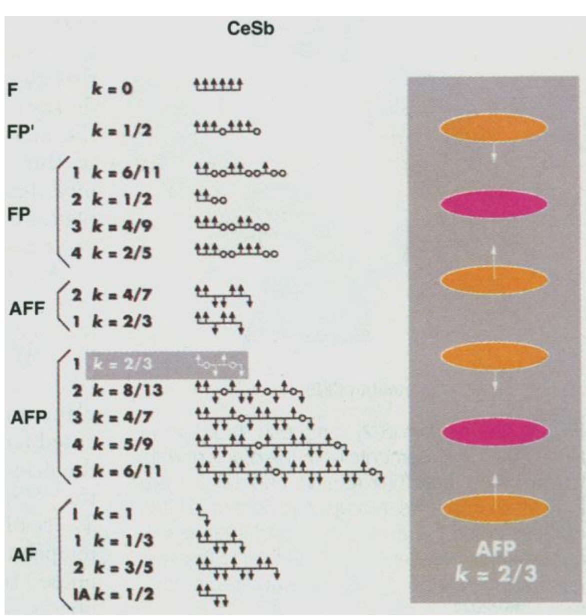

Fig. 6. Schematic diagram of the modulated magnetic phases in CeSb. The arrows and open circles (zeros) represent ferromagnetic and nonmagnetic (001) planes, respectively. In the ferromagnetic planes, the magnetic moments are parallel to the c axis, that is, perpendicular to the (001) planes. The modulation is also along the c axis. In the schematic diagram, the spins are shown perpendicular to the modulation direction for clarity, but their orientations are really parallel to this direction. The modulations are commensurate with the lattice and are square-wave type; that is, the magnetic moments have constant values. On the right, a more realistic diagram of the magnetic structure of the AFP phase with $k_z = 2/3$ is shown as an example.

bands is taken into account, has been developed by Kasuya and his co-workers (36). This model is very successful in explaining the anomalous magnetic properties of CeSb and CeBi. A delicate balance between the crystal field splitting and the strength of the p-f hybridization is responsible for the existence of the modulated phases with nonmagnetic planes in CeSb. Hydrostatic pressure destabilizes this delicate balance and leads to the disappearance of such phases.

Related Areas

The complementary use of neutron and x-ray magnetic scattering techniques is extremely powerful for the study of magnetic materials. The experimental results for magnetic structures in rare earth metallic systems are established, and our theoretical understanding is quite reasonable, although not complete. Recently, a number of magnetic phases have been discovered in heavy fermion and high-temperature superconducting materials. These materials form a class of strongly correlated electron systems for which there is a possible interplay between magnetic interactions and superconductivity. These materials certainly merit a separate article.

REFERENCES AND NOTES

1. F. Bloch, *Phys. Rev.* **50**, 259 (1936).
2. L. W. Alvarez and F. Bloch, *ibid.* **57**, 111 (1940).
3. O. Halperin and M. H. Johnson, *ibid.* **55**, 898 (1939).
4. L. Néel, *Ann. Phys. (Paris)* **17**, 5 (1932); *ibid.* **3**, 137 (1948).
5. C. G. Shull and J. S. Smart, *Phys. Rev.* **76**, 1256 (1949).
6. G. L. Squires, *Thermal Neutron Scattering* (Cambridge Univ. Press, Cambridge, 1978).
7. S. W. Lovesey, *Theory of Neutron Scattering from Condensed Matter* (Oxford Univ. Press, London, 1984).
8. ———, *Rep. Prog. Phys.* **56**, 257 (1993).
9. A. Herpin and P. Mériel, *J. Phys. (Paris)* **22**, 337 (1961); ——— and J. Villain, *C. R. Acad. Sci.* **249**, 1334 (1959).
10. A. Yoshimori, *J. Phys. Soc. Jpn.* **14**, 807 (1959).
11. R. A. Erickson, *Phys. Rev.* **90**, 779 (1953).
12. W. C. Koehler, J. W. Cable, E. O. Wollan, M. K. Wilkinson, *J. Phys. Soc. Jpn. B III* **17**, 32 (1962); W. C. Koehler, in *Magnetic Properties of Rare Earth Metals*, R. J. Elliot, Ed. (Plenum, New York, 1972), chap. 3, p. 81; ———, J. W. Cable, H. R. Child, M. K. Wilkinson, E. O. Wollan, *Phys. Rev.* **158**, 450 (1967).
13. G. Shirane and W. J. Takei, *J. Phys. Soc. Jpn. BIII* **17**, 35 (1962).
14. E. Fawcett, *Rev. Mod. Phys.* **60**, 209 (1988), and references therein.
15. Yu. A. Izyumov, *Sov. Phys. Usp.* **27**, 845 (1984).
16. J. Rossat-Mignod, in *Methods of Experimental Physics*, K. Sköld and D. L. Price, Eds. (Academic Press, New York, 1987), vol. 23, part C, p. 69.
17. T. Chattopadhyay, *Int. J. Mod. Phys. B* **7**, 3225 (1993).
18. W. Selke, *Phys. Rep.* **170**, 213 (1988), and references therein; J. Yeomans, in *Solid State Physics* (Academic Press, New York, 1988), vol. 41, p. 151, and references therein.
19. J. Jensen and A. R. Mackintosh, *Rare Earth Magnetism* (Oxford Univ. Press, Oxford, 1991); J. Jensen and A. R. Mackintosh, *J. Magn. Magn. Mater.* **104–107**, 1481 (1992).
20. The periodicity of a magnetic structure is expressed in physical or direct space by the repeat distance (or the number of atomic layers) of the modulation wave. Physicists and crystallographers often use reciprocal, momentum, or wave-vector space. The physical realization of such a space is the space generated by the scattered beam. If **a**, **b**, and **c** define the direct lattice, then their reciprocals **a***, **b***, and **c*** define the reciprocal lattice, which gives the positions of the nuclear Bragg peaks. The positions of the magnetic peaks of the antiferromagnetic structures or the positions of the satellite reflections of the modulated structures can be generated by the wave vector **k** from the reciprocal lattice vector $\mathbf{H} = h\mathbf{a}^* + k\mathbf{b}^* + l\mathbf{c}^*$ (h, k, and l are the Miller indices) by the relation $\mathbf{G} = \mathbf{H} \pm \mathbf{k}$. For a simple antiferromagnetic structure, the wave vector components are simple fractions, namely, $\mathbf{k} = (1/2, 1/2, 1/2)$. For a modulated structure, the components have in general nonrational values. For rare earth metals, the wave vectors of the modulated phases are given by $k = (0, 0, k_z)$, where k_z is expressed in units of c^*.
21. D. Gibbs, *J. Less Common Metals* **148**, 109 (1989).
22. ———, D. E. Moncton, K. L. D'Amico, J. Bohr, B. H. Grier, *Phys. Rev. Lett.* **55**, 234 (1985).
23. J. Bohr, D. Gibbs, D. E. Moncton, K. L. D'Amico, *Physica A* **140**, 349 (1986).
24. R. A. Cowley and S. Bates, *J. Phys. C* **21**, 4113 (1988).
25. A. R. Mackintosh and J. Jensen, in *Disorder in Condensed Matter Physics*, J. A. Blackman and J. Taguena, Eds. (Oxford Univ. Press, Oxford, 1991), p. 214.
26. J. Jensen and A. R. Mackintosh, *Phys. Rev. Lett.* **64**, 2699 (1990).
27. D. A. Jehan, D. F. McMorrow, R. A. Cowley, G. J. McIntyre, *Europhys. Lett.* **17**, 553 (1992).
28. J. von Boehm and P. Bak, *Phys. Rev. Lett.* **42**, 122 (1979); see also P. Bak and J. von Boehm, *Phys. Rev. B* **21**, 5297 (1980).
29. J. Rossat-Mignod *et al.*, *J. Magn. Magn. Mater.* **52**, 111 (1985), and references therein.
30. B. Hälg, A. Furrer, W. Hälg, O. Vogt, *J. Phys. C* **14**, L961 (1981).
31. T. Chattopadhyay *et al.*, *J. Magn. Magn. Mater.* **54–57**, 503 (1986).
32. T. Chattopadhyay *et al.*, *ibid.* **63**, **64**, 52 (1987).
33. K. Takegahara, H. Takahashi, A. Yanase, T. Kasuya, *Solid State Commun.* **39**, 857 (1981).
34. K. Nakanishi, *J. Phys. Soc. Jpn.* **58**, 1296 (1989).
35. L. P. Regnault *et al.*, *Physica B* **156**, **157**, 798 (1989).
36. H. Takahashi and T. Kasuya, *J. Phys. C* **18**, 2697 (1985); *ibid.*, pp. 2709, 2721, 2731, 2745, and 2755.

37. I thank my colleagues B. Chakraverty, S. Mason, A. Murani, and C. Wilkinson for the critical reading of the manuscript.

RESEARCH ARTICLE

Neural Mechanisms for Forming a Perceptual Decision

C. Daniel Salzman and William T. Newsome*

Cognitive and behavioral responses to environmental stimuli depend on an evaluation of sensory signals within the cerebral cortex. The mechanism by which this occurs in a specific visual task was investigated with a combination of physiological and psychophysical techniques. Rhesus monkeys discriminated among eight possible directions of motion while directional signals were manipulated in visual area MT. One directional signal was generated by a visual stimulus and a second signal was introduced by electrically stimulating neurons that encoded a specific direction of motion. The decisions made by the monkeys in response to the two signals allowed a distinction to be made between two possible mechanisms for interpreting directional signals in MT. The monkeys tended to cast decisions in favor of one or the other signal, indicating that the signals exerted independent effects on performance and that an interactive mechanism such as vector averaging of the two signals was not operative. Thus, the data suggest a mechanism in which monkeys chose the direction encoded by the largest signal in the representation of motion direction, a "winner-take-all" decision process.

Within the cerebral cortex, the visual environment is encoded by the electrical activity of neurons in topographically organized maps of visual space. Little is known, however, about how the neuronal signals within a sensory representation are interpreted to form perceptual decisions that guide behavior. Such decision processes have been extensively modeled in cognitive psychology and psychophysics to provide quantitative accounts of human performance in a variety of discrimination tasks (1). Physiological approaches that test and refine such models are essential for understanding the neural basis of cognitive behavior. Here we describe a physiological experiment that explores how sensory sig-

The authors are in the Department of Neurobiology, Stanford University School of Medicine, Stanford, CA 94305, USA.

*To whom correspondence should be addressed.